

Relationship of Calcium Transients to Calcium Currents and Charge Movements in Myotubes Expressing Skeletal and Cardiac Dihydropyridine Receptors

JESÚS GARCÍA, TSUTOMU TANABE and KURT G. BEAM

From the Department of Physiology, Colorado State University, Fort Collins, Colorado 80523

ABSTRACT In both skeletal and cardiac muscle, the dihydropyridine (DHP) receptor is a critical element in excitation-contraction (e-c) coupling. However, the mechanism for calcium release is completely different in these muscles. In cardiac muscle the DHP receptor functions as a rapidly-activated calcium channel and the influx of calcium through this channel induces calcium release from the sarcoplasmic reticulum (SR). In contrast, in skeletal muscle the DHP receptor functions as a voltage sensor and as a slowly-activating calcium channel; in this case, the voltage sensor controls SR calcium release. It has been previously demonstrated that injection of dysgenic myotubes with cDNA (pCAC6) encoding the skeletal muscle DHP receptor restores the slow calcium current and skeletal type e-c coupling that does not require entry of external calcium (Tanabe, Beam, Powell, and Numa. 1988. *Nature*. 336:134–139). Furthermore, injection of cDNA (pCARD1) encoding the cardiac DHP receptor produces rapidly activating calcium current and cardiac type e-c coupling that does require calcium entry (Tanabe, Mikami, Numa, and Beam. 1990. *Nature*. 344:451–453). In this paper, we have studied the voltage dependence of, and the relationship between, charge movement, calcium transients, and calcium current in normal skeletal muscle cells in culture. In addition, we injected pCAC6 or pCARD1 into the nuclei of dysgenic myotubes and studied the relationship between the restored events and compared them with those of the normal cells. Charge movement and calcium currents were recorded with the whole cell patch-clamp technique. Calcium transients were measured with Fluo-3 introduced through the patch pipette. The kinetics and voltage dependence of the charge movement, calcium transients, and calcium current in dysgenic myotubes expressing pCAC6 were qualitatively similar to the ones elicited in normal myotubes: the calcium transient displayed a sigmoidal dependence on voltage and was still present after the addition of 0.5 mM Cd²⁺ + 0.1 mM La³⁺. In contrast, the calcium transient in dysgenic myotubes expressing pCARD1 followed the amplitude of the calcium

Dr. Tanabe's present address is Howard Hughes Medical Institute, Department of Cellular and Molecular Physiology, Yale University, New Haven, CT 06536.

Address correspondence to Kurt G. Beam, Department of Physiology, Colorado State University, Fort Collins, CO 80523.

current and thus showed a bell shaped dependence on voltage. In addition, the transient had a slower rate of rise than in pCAC6-injected myotubes and was abolished completely by the addition of $\text{Cd}^{2+} + \text{La}^{3+}$.

INTRODUCTION

In the contraction of both skeletal and cardiac muscle cells, a key event is the release of calcium from the sarcoplasmic reticulum (SR), which is elicited as a consequence of depolarization of the plasmalemma. In this process, termed excitation-contraction (e-c) coupling, an essential plasmalemmal protein is the dihydropyridine (DHP) receptor (Ríos and Brum, 1987; Tanabe, Beam, Powell, and Numa, 1988). Although the DHP receptor is present in both skeletal and cardiac muscle, the mechanism controlling the release of calcium from the SR is different in the two cell types. In cardiac muscle the DHP receptor functions as a calcium channel which, upon depolarization of the membrane, activates with a fast time course to allow the influx of calcium ions into the cell. This calcium influx triggers the opening of the SR calcium release channel (Fabiato, 1985; Näbauer, Callewaert, Cleemann, and Morad, 1989). In skeletal muscle, the DHP receptor is thought to have a dual role, functioning both as a slowly activating calcium channel and as the voltage sensor that controls SR calcium release (Ríos and Brum, 1987; Tanabe et al., 1988). The concept of a voltage sensor was first suggested by Schneider and Chandler (1973), who proposed that this structure produced the nonlinear capacitative current, termed charge movement, which they found to be present in skeletal muscle. Additionally, the possibility was suggested that a mechanical linkage between the voltage sensor and the SR could control the release of calcium from the latter structure (Chandler, Rakowski, and Schneider, 1976).

Muscular dysgenesis (*mdg*) is a fatal, autosomal, recessive mutation (Gluecksohn-Waelsch, 1963) that causes the failure of e-c coupling in skeletal muscle (Powell and Fambrough, 1973; Klaus, Scordilis, Rapalus, Briggs, and Powell, 1983). Electrophysiologically, dysgenic muscle has been shown to lack slowly activating calcium current (Beam, Knudson, and Powell, 1986) and to have a greatly reduced amount of intramembrane charge movement (Adams, Tanabe, Mikami, Numa, and Beam, 1990; Shimahara, Bournaud, Inoue, and Strube, 1990). The *mdg* mutation alters the gene that encodes the skeletal muscle DHP receptor (Tanabe et al., 1988; Chaudhari, 1992) with the result that the translation product of the gene is absent (Knudson, Chaudhari, Sharp, Powell, Beam, and Campbell, 1989). This absence appears to account for the phenotypic abnormalities of dysgenic muscle because e-c coupling, slow calcium current (Tanabe et al., 1988) and intramembrane charge movement (Adams et al., 1990) can be restored by the injection of an expression plasmid which encodes the skeletal muscle DHP receptor.

Because other proteins involved in e-c coupling, including calsequestrin, the ryanodine receptor (postulated to be the SR calcium release channel) and the $\text{Ca}^{2+}/\text{Mg}^{2+}$ ATPase of the SR, are present in skeletal muscle from dysgenic mice (Knudson et al., 1989), cultured dysgenic muscle provides an excellent environment for expressing DHP receptors in order to study their interaction with the SR release channel. Previous studies of DHP receptors expressed in dysgenic muscle (Tanabe et al., 1988, 1990a,b; Adams et al., 1990) have measured electrical signals associated with the DHP receptor (ionic current, intramembrane charge movement), but have

only monitored intracellular calcium release very indirectly, by means of electrically evoked contractions. In this paper, we have used calcium indicator dyes to obtain a more direct measurement of intracellular calcium release. The calcium transients were recorded during voltage clamp measurements of calcium current or intramembrane charge movement in cultured normal myotubes or dysgenic myotubes injected with plasmids that encode the DHP receptor of either skeletal (pCAC6) or cardiac muscle (pCARD1). This has allowed us to obtain a quantitative description of the relationship between the calcium transients and these membrane currents. Preliminary reports of some of the results have appeared (García, Tanabe, and Beam, 1993; Beam and García, 1993).

MATERIALS AND METHODS

Electrical and Optical Measurements

Transmembrane currents were recorded using the whole-cell configuration of the patch-clamp technique (Hamill, Marty, Neher, Sakmann, and Sigworth, 1981). Calcium transients were measured with the fluorescent indicator dye Fluo-3 (Molecular Probes, Inc., Eugene, OR), which was loaded into cells as the pentapotassium salt contained in the whole-cell patch pipette. Additional details on recording procedures are described in the preceding paper (García and Beam, 1994). The prepulse protocol (Adams et al., 1990) was used as voltage clamp command sequence for the measurement of both calcium currents and charge movement. In this protocol, voltage is first stepped from the holding potential (-80 mV) to -30 or -40 mV for 1 s and then to -50 mV for 25–30 ms, varying test potentials for 15 ms, -50 mV for 25–30 ms, and finally back to the holding potential again. The purpose of this protocol was to inactivate ionic currents through sodium and T-type calcium channels, and to cause immobilization of intramembrane charge movements associated with these two channel types, before the 15-ms test pulses. Voltage clamp command sequences were applied every 20 s.

Electrical and optical signals were sampled simultaneously at either 4 or 10 kHz. Analog filtering was set at 2 kHz for the electrical recordings and at 0.1–1 kHz for the optical recordings. All the records shown are single traces for both membrane currents and calcium transients.

Injection and Expression of the Plasmids

Nuclei of dysgenic myotubes were microinjected with the expression plasmids pCAC6 or pCARD1 on the sixth to seventh day after initial plating of myoblasts into primary culture. Both the procedures for microinjection and for tissue culture were essentially as described in Tanabe et al. (1988). The expression plasmids carry cDNA inserts encoding the rabbit skeletal muscle (pCAC6; Tanabe et al., 1988) or the rabbit cardiac muscle (pCARD1; Mikami, Imoto, Tanabe, Niidome, Mori, Rakeshima, Narumiya, and Numa, 1989) DHP receptor. The concentration of the cDNA in the injection pipette was 0.5 $\mu\text{g}/\mu\text{l}$ for pCAC6 and 0.5 – 1 $\mu\text{g}/\mu\text{l}$ for pCARD1. Myotubes were examined 2–4 d after the injection. Myotubes expressing the skeletal muscle or cardiac DHP receptors were identified by contractions evoked by electrical stimulation (80 V, 5-ms pulses) applied via a blunt tipped (5 μm) extracellular pipette positioned near (<50 μm) the cell as described earlier (Tanabe et al., 1988; 1990*a,b*).

Solutions

Patch pipettes were made from borosilicate glass and had resistances of 1.6–2.1 M Ω when filled with "internal solution," which contained (mM): 145 Cs-aspartate, 10 HEPES, 5 Mg₂Cl, 0.1 Cs₂EGTA, and 0.2 K₅Fluo-3. The external solution contained (mM): 145 TEACl, 10 HEPES, 10

CaCl₂, and 0.003 TTX. For the measurement of intramembrane charge movement, 0.5 mM CdCl₂ and 0.1 mM LaCl₃ were added to this external solution. The pH of all solutions was adjusted to 7.4 with CsOH.

The bath volume of the recording chamber was ~0.5 ml. The bath was exchanged with at least 20 ml of any new solution. Temperature (22–24°C) was monitored with a thermistor probe placed within the recording chamber. Data are presented as mean ± SEM, with the number of experiments in parentheses.

RESULTS

Calcium Transients and Slow Calcium Current in Normal Myotubes

Fig. 1 shows the calcium transients and the slow calcium current elicited from a normal myotube by test pulses (15 ms in duration) to the membrane potentials indicated next to the traces. Because the prepulse protocol was used (see Materials and Methods), the recorded current represents the slow, dihydropyridine-sensitive calcium current with little contamination from other currents. For this particular cell, the current was detected at 0 mV, became larger and reached a maximum at 30 mV. The maximum amplitude of the calcium current for different cells (10 mM external calcium concentration) was -2.7 ± 0.3 pA/pF ($n = 31$), measured at the end of the 15-ms pulses. As described in the previous paper, the calcium transient was usually detectable for weaker depolarizations than the calcium current and rose more rapidly and had a larger amplitude for stronger depolarizations. The average, maximal $\Delta F/F$ value for the calcium transient was 1.8 ± 0.5 ($n = 31$), also measured at the end of the 15-ms pulse. Note that the amplitude of the slow calcium current first increased and then decreased for stronger depolarizations (as the test depolarization approached the reversal potential), while the amplitude of the calcium transient increased monotonically to a saturating level at test potentials greater than ≈ 30 mV.

Lack of Calcium Transients in Dysgenic Myotubes

Because dysgenic myotubes do not contract under ordinary conditions in response to depolarization (Klaus et al., 1983; Tanabe et al., 1988), they would appear to provide an excellent “null background” for studying calcium transients produced by exogenous DHP receptors introduced by injection of appropriate cDNAs. However, consideration must be given to the fact that dysgenic myotubes express a low density of an L-type calcium current, termed I_{dys} , that differs from the slow calcium current of normal myotubes in several respects, including faster activation kinetics and a higher sensitivity to DHPs (Adams and Beam, 1989). Furthermore, it has been shown that after I_{dys} has been potentiated by a DHP agonist (1 μM Bay K 8644), some dysgenic myotubes do display depolarization-induced contractions that depend upon the entry of extracellular calcium (Adams and Beam, 1991). This result raises the possibility that in the absence of the DHP agonist, I_{dys} may trigger elevations of intracellular calcium that are subthreshold for eliciting a visible contraction. To investigate this possibility, we examined the effect of depolarization on intracellular calcium levels in control dysgenic myotubes that had not been injected with the cDNAs that encode the skeletal muscle or cardiac DHP receptor. Altogether, we analyzed eleven dysgenic

myotubes in which the density of I_{dys} averaged 0.53 ± 0.12 pA/pF, similar to the value of 0.48 pA/pF found by Adams and Beam (1991) under comparable conditions. Fig. 2 illustrates the results obtained from the dysgenic myotube out of this group of eleven that displayed the largest I_{dys} , with a maximum amplitude of almost 1 pA/pF. In this cell, 15-ms depolarizations to potentials ≤ 20 mV did not elicit detectable calcium transients. A depolarization to +30 mV did elicit a small transient (maximal $\Delta F/F$ of 0.04), which had a very long delay with respect to the onset of the

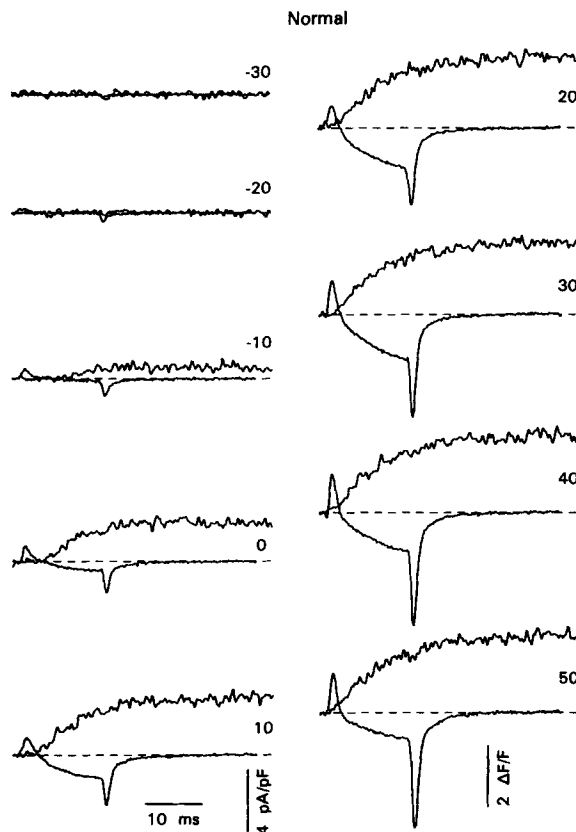


FIGURE 1. Calcium transient and calcium current in a normal myotube. In this and all subsequent figures, the membrane potential during the test pulse (15-ms duration) is indicated by the number at the right. Unless otherwise noted, the onset of the test pulses occurred 0.5 ms from the beginning of the illustrated traces. At each test potential, the calcium transient is the noisier trace which remains at or above the dashed baseline. Note that a small calcium transient was elicited by a weaker depolarization (-10 mV) than that required to elicit inward calcium current (0 mV). Because the calcium current of normal myotubes is very slowly activating, the inward current is still increasing at the end of the 15-ms test pulses. Measured at the end of the test pulse, the amplitude of the current first increased with increasing test depolarization and then decreased again for potentials

> 30 mV. The calcium transient became larger and rose more quickly with increasing depolarization up to about +30 mV, beyond which it remained roughly constant.

depolarization. The average maximal $\Delta F/F$ elicited by 15 ms test pulses averaged 0.01 ± 0.01 ($n = 11$). The calcium transient was slightly more prominent when 100- to 200-ms test depolarizations were used (not shown), but still very small (maximal $\Delta F/F$ of 0.02 ± 0.02 , $n = 6$). In conclusion, for the 15-ms test pulses that we routinely used, it seems unlikely that elevations of myoplasmic calcium caused by endogenous I_{dys} contributed significantly to the calcium transients in dysgenic myotubes expressing pCAC6 or pCARD1 (see below).

Calcium Transients and Slow Calcium Current in Dysgenic Myotubes Expressing pCAC6

Previously it was shown that injection of dysgenic myotubes with the expression plasmid pCAC6 restores spontaneous and electrically evoked contractions as well as slow calcium current (Tanabe et al., 1988). Fig. 3 illustrates calcium transients and calcium currents from a dysgenic myotube injected with pCAC6. As in normal myotubes (García and Beam, 1994), an appreciable calcium transient generally could be elicited by a weaker depolarization (e.g., -10 mV in Fig. 3) than that required (0

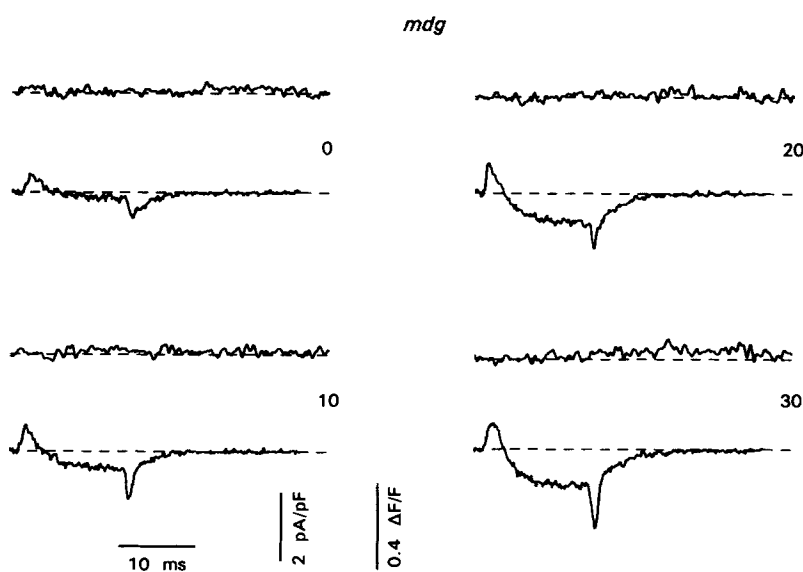


FIGURE 2. Absence of calcium transient and slowly activating calcium current in dysgenic myotubes. At each of the indicated test potentials, the calcium transient is illustrated on the upper baseline and the membrane current on the lower baseline. In the current traces, the prominent outward deflection at the onset of the test depolarization (due to immobilization-resistant charge movement) is followed by a small, inward calcium current, I_{dys} . I_{dys} reaches a steady-state level within less than 10 ms, thus distinguishing it from the much more slowly activating calcium current of normal myotubes (compare with Fig. 1). Note the absence of a calcium transient at all test potentials except for a small fluorescence change that occurs after repolarization from $+30$ mV.

mV in Fig. 3) to elicit an appreciable slow calcium current. Also as in normal myotubes, the calcium transient became larger and faster with stronger depolarizations and saturated in amplitude for potentials of $\sim +40$ mV and above. The average amplitude of the maximal $\Delta F/F$ was 1.0 ± 0.2 ($n = 19$) in 10 mM external calcium. The slow calcium current in pCAC6-injected myotubes had activation kinetics resembling those of the slow calcium current of normal myotubes, although the maximum amplitude of the expressed current, for a 15-ms test pulse, was $\sim 1.3 \pm 0.3$ pA/pF ($n = 22$), about half that of normal myotubes. Consistent with the idea that

the DHP receptor can function both as a voltage sensor controlling SR calcium release and as a slowly-activating calcium channel (Tanabe et al., 1988), all the injected myotubes that contracted in response to electrical stimulation displayed both a calcium transient and a slow calcium current.

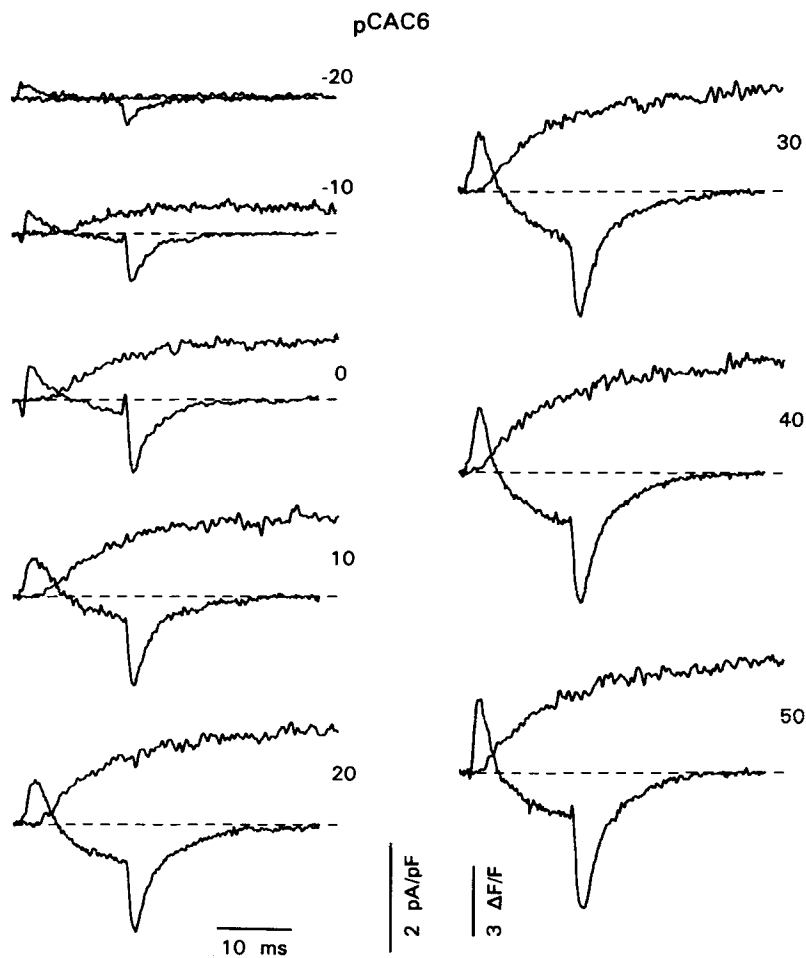


FIGURE 3. Calcium transient and slow calcium current in dysgenic myotubes injected with pCAC6. The calcium transient and slow calcium current were restored by injection (2 d before recording) of this dysgenic myotube with the expression plasmid pCAC6, which encodes the rabbit skeletal muscle DHP receptor. The calcium transient and the slow calcium current restored by pCAC6 resembled those from normal myotubes (Fig. 1).

Cardiac-Type Calcium Transient and Calcium Current Restored by pCARD1

Injection of the expression plasmid pCARD1 can also restore contraction of dysgenic myotubes, although in this case the contraction depends on calcium entry (Tanabe et al., 1990a). Fig. 4A shows the calcium transient and the calcium current recorded

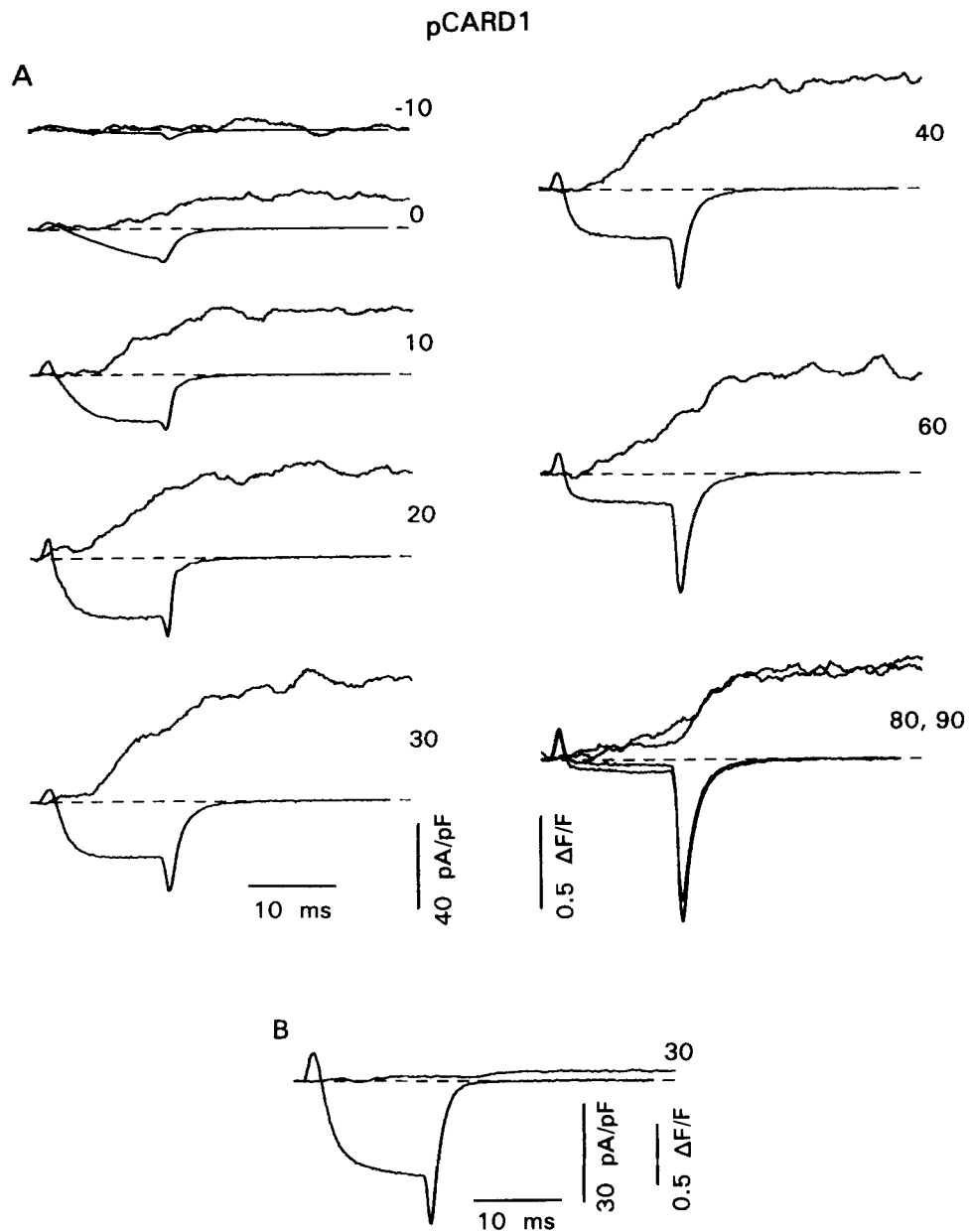


FIGURE 4. Calcium transient and calcium current in dysgenic myotubes injected with pCARD1. Dysgenic myotubes were injected two days before recording with the expression plasmid pCARD1, which encodes the cardiac muscle DHP receptor. (A) Cardiac-like calcium current and calcium transient in a pCARD1-injected myotube. The calcium current activates with much faster kinetics than in normal (Fig. 1) or pCAC6-injected (Fig. 3) myotubes, reaching a steady state level in <10 ms for test potentials >10 mV. The calcium transient rises more slowly than in normal or pCAC6-injected myotubes. It also differs in that it follows the amplitude of the calcium current. Thus, at the end of the 15-ms test pulse, the amplitude of the

from a dysgenic myotube injected with pCARD1. The expressed calcium current activated much more rapidly, reaching a steady amplitude within 15 ms for test potentials > 20 mV, than the current in normal myotubes or in dysgenic myotubes expressing pCAC6, which was still increasing at the end of the 15-ms test pulse (compare Figs. 1, 3, and 4A). The average amplitude of the peak current in pCARD1-expressing myotubes was -26.4 ± 2.2 pA/pF ($n = 17$). The calcium transient in dysgenic myotubes expressing pCARD1 (measured at the end of the 15-ms test pulse) first became appreciable in response to a test depolarization of either the same magnitude as that required to elicit appreciable calcium current (e.g., 0 mV in Fig. 4A) or, more commonly, for a test depolarization about 10 mV larger. This is in contrast to both normal myotubes and dysgenic myotubes expressing pCAC6, in which a weaker depolarization was required to elicit an appreciable calcium transient than was necessary for evoking a detectable slow calcium current. Another important difference is that in normal myotubes and pCAC6-expressing dysgenic myotubes the amplitude of the calcium transient increased monotonically as a function of test potential, whereas in pCARD1-injected myotubes the transient initially increased in amplitude for increasing test depolarizations, reached a maximum (at +30 mV in Fig. 4A) and then decreased again for still stronger depolarizations. Thus, the amplitude of the calcium transient in pCARD1-injected myotubes mirrors the amplitude of the calcium current. This was particularly evident for very strong depolarizations. For example, when a pCARD1-injected cell was depolarized to near the reversal for calcium current (e.g., +80 or +90 mV for the cell in Fig. 4A), both the current and the calcium transient were small during the test pulse. Upon repolarization, however, there was a large increase in both the calcium current and the calcium transient. In dysgenic myotubes expressing the cardiac DHP receptor, the relationship between the amplitudes of the calcium current and calcium transient, and their dependence on test potential, are similar to their behavior in cardiac muscle (Beuckelman and Wier, 1988; Näbauer et al., 1989; Wier, 1990). The maximum amplitude of the calcium transient ($\Delta F/F$) in pCARD1-injected cells, measured at the end of the 15-ms test pulses, was only 0.33 ± 0.06 ($n = 17$), about four- or fivefold smaller than in pCAC6-injected or normal myotubes, respectively (Table I, column 4). If it is assumed that resting calcium was similar in the pCARD1- and pCAC6-injected myotubes, then the difference in $\Delta F/F$ suggests that the cardiac DHP receptor is less effective than the skeletal muscle DHP receptor in eliciting calcium release in skeletal muscle cells.

All pCARD1-injected dysgenic myotubes that contracted in response to electrical stimulation were found to display both a calcium current and a calcium transient, as illustrated for the cell in Fig. 4A. However, some pCARD1-injected cells that displayed either a very weak contraction, or no contraction at all, nonetheless expressed a high density of L-type calcium current (Fig. 4B; Discussion).

transient and current increase and then decrease in parallel for increasing test depolarization. At any given test pulse, the transient shows an increase (particularly noticeable at +80 and +90 mV) that coincides with the large, inward tail of calcium current that occurs when potential is repolarized at the end of the test pulse. (B) Example of a cell in which injection of pCARD1 resulted in a large current but only a very small transient. A single pulse to 20 mV is shown.

Voltage Dependence of the Calcium Transient and the Calcium Current

Fig. 5 shows the dependence on test potential of calcium current (●) and the normalized fluorescence change (▲) in a representative normal myotube (*left*), a pCAC6-injected myotube (*center*), and a pCARD1-injected myotube (*right*). For all three, the curve relating current to test potential is U-shaped. In normal and pCAC6-injected myotubes, the curve relating the fluorescence change to test potential is S-shaped, whereas for the pCARD1-injected myotubes this curve has an inverted U shape. For the current, the data have been fitted with the smooth curve

$$I = G'_{\max} (V - V_{\text{rev}}) / [1 + \exp \{(V'_{\text{G}}(1/2) - V) / k'_{\text{G}}\}], \quad (1)$$

where G'_{\max} is the maximum conductance for a 15-ms test pulse, V_{rev} is the reversal potential (determined as one of the fitted parameters), V is the test potential, $V'_{\text{G}}(1/2)$ is

TABLE I
Average Values of Fitted Parameters in Normal and Injected Myotubes

	10 Ca						10 Ca + 0.5 Cd + 0.1 La					
	1 G'_{\max}	2 $V'_{\text{G}}(1/2)$	3 k'_{G}	4 $\Delta F/F_{\max}$	5 $V_{\text{F}}(1/2)$	6 k_{F}	7 Q_{\max}	8 $V_{\text{Q}}(1/2)$	9 k_{Q}	10 $\Delta F/F_{\max}$	11 $V_{\text{F}}(1/2)$	12 k_{F}
	nS/nF	mV	mV		mV	mV	nC/ μ F	mV	mV		mV	mV
Normal	104 ± 17 (30)	17 ± 0.9 (30)	6.6 ± 0.3 (30)	1.8 ± 0.5 (31)	4.1 ± 0.9 (31)	7.7 ± 0.4 (31)	5.1 ± 0.9 (6)	1.4 ± 0.9 (6)	12.7 ± 1.5 (6)	1.0 ± 0.3 (6)	13.0 ± 2.2 (6)	6.6 ± 0.7 (6)
pCAC6	49 ± 8.8 (17)	24 ± 2.6 (17)	8.2 ± 0.5 (17)	1.0 ± 0.2 (19)	6.6 ± 0.9 (19)	9.0 ± 0.6 (19)	4.6 ± 0.5 (4)	-3.5 ± 2.5 (4)	14.0 ± 0.8 (4)	0.6 ± 0.1 (10)	6.9 ± 1.5 (10)	8.2 ± 0.6 (10)
pCARD1	319* ± 76 (4)	6.6* ± 1.7 (4)	5.0* ± 0.3 (4)	0.3 [‡] ± 0.1 (18)	—	—	13.6 ± 2.1 (8)	-0.6 ± 0.8 (8)	13.3 ± 0.7 (8)	0 [§]	—	—

*Data shown only for cells with estimated series resistance error ≤ 10 mV (average of 5.9 ± 1.4 mV); for cells with an error ≤ 15 mV ($n = 10$), $G'_{\max} = 329 \pm 39$ nS/nF, $V'_{\text{G}}(1/2) = 4.9 \pm 1.0$ mV, $k'_{\text{G}} = 4.4 \pm 0.3$ mV. [‡]Maximum value obtained without fitting to a sigmoidal curve. [§]Blocking the current eliminated the calcium transient.

the potential that elicits the half-maximal increase in conductance, and k'_{G} is a steepness parameter. For the fluorescence, the data have been fitted with the smooth curve

$$\frac{\Delta F/F}{(\Delta F/F)_{\max}} = 1 / [1 + \exp \{(V_{\text{F}}(1/2) - V) / k_{\text{F}}\}], \quad (2)$$

where $(\Delta F/F)_{\max}$ is the maximum fluorescence change, $V_{\text{F}}(1/2)$ is the potential that elicits the half-maximal increase in fluorescence change, and V and k_{F} have meanings as above. Average values for the fitted parameters (except V_{rev}) are summarized in Table I (columns 1–6). Note that for pCARD1-injected myotubes, no values are given for $V_{\text{F}}(1/2)$ or k_{F} because the fluorescence change vs potential curve is not described by Eq. 2. Also, in the case of the pCARD1-injected myotubes, the large size of the expressed current (2.2–43.5 nA/cell) and the resulting series resistance error would

be expected to have the effect of shifting $V_G^{1/2}$ in the hyperpolarizing direction and causing the value of k_G to be too small; thus, Table I gives values for these parameters only for the subset of pCARD1-injected myotubes in which the estimated series resistance error ($I_{max} \cdot R_{series}$) was comparatively small. Calculation of $V_G^{1/2}$ and k_G was less problematic in normal and pCAC6-injected myotubes, since both the slow calcium current and estimated series resistance error was relatively small in these cells. It has been reported that the voltage-dependence for activation of slow calcium current differs between normal and pCAC6-injected myotubes (Adams et al., 1990). This was also apparent in our experiments in that the value of $V_G^{1/2}$ for pCAC6-injected myotubes was shifted toward the right 7 mV compared to $V_G^{1/2}$ for normal

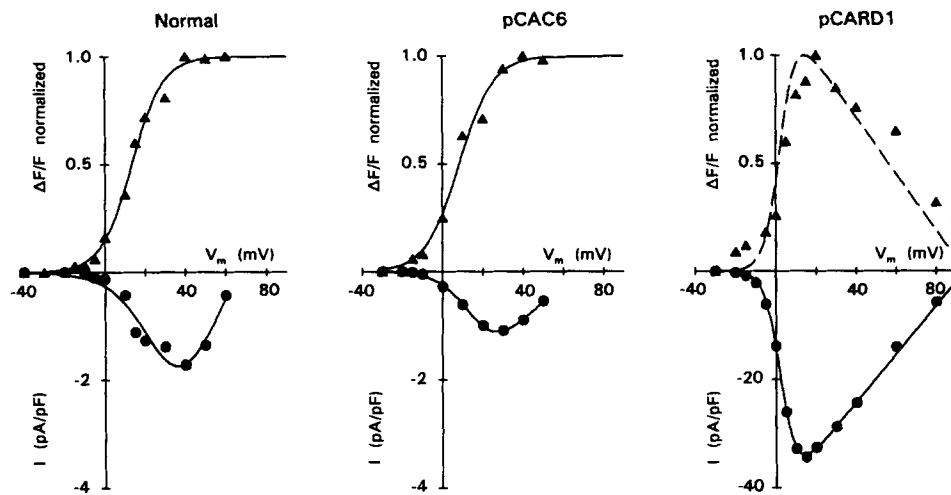


FIGURE 5. Comparison of voltage dependence of calcium currents and calcium transients. The amplitude of calcium current (●) and calcium transient (▲) is plotted as a function of test potential for a representative normal myotube (*left*), pCAC6-injected myotube (*middle*), and pCARD1-injected myotube (*right*). The calcium currents are normalized by linear cell capacitance and the calcium transient to the maximum amplitude for each cell. Smooth curves represent least-squares fits of Eqs. 1 or 2 for the current and transient data, respectively. The broken curve through the calcium transient data for the pCARD1-injected cell, was obtained by inverting, and normalizing to one, the smooth curve through the current data.

myotubes. In contrast to conductance, $V_F^{1/2}$ for the fluorescence change (Table I, column 5) was much more similar for normal and pCAC6-injected myotubes, differing by only 2.5 mV.

The differences in the amplitudes of the calcium current between the three types of myotubes are reflected in the values of G'_{max} for each (normal, 104 nS/nF; pCAC6, 49 nS/nF; pCARD1, 329 nS/nF). Our value of G'_{max} for pCARD1 is close to the value of G_{max} (488 nS/nF) found by Adams et al. (1990), whereas the values of G'_{max} for normal and pCAC6-injected myotubes are much smaller than the previously reported values of G_{max} (normal, 459 nS/nF; pCAC6, 141 nS/nF). In large part, this difference can be accounted for by the fact that the calcium currents in normal and pCAC6-

injected myotubes have such slow kinetics that they were much less completely activated by the 15-ms test pulses used in the present study than by the 200-ms test pulses used in the earlier study. Note that in addition to having a larger value of G'_{\max} , pCARD1-injected myotubes had a more negative value of $V_G^{1/2}$ (Table I), which also contributes to the larger size of the expressed current in these cells.

Comparison on a Long Time Base of the Calcium Transients in pCAC6- and pCARD1-Injected Myotubes

Fig. 6 illustrates 1.2-s recordings of the calcium transients elicited by 15-ms depolarizations applied to myotubes injected with either pCAC6 (*A*) or pCARD1 (*B*). In the pCAC6-injected myotube, the transient in response to a depolarization of -10 mV began to decay shortly after repolarization, whereas the transients in response to depolarizations of $+10$ and $+30$ mV continued to increase slowly for several tens of ms after the depolarization was terminated. This behavior of the transients is similar to that reported for normal myotubes in the previous paper (García and Beam, 1994). Although the possibility of dye saturation could not be excluded, it was suggested that (*a*) the primary control of intracellular calcium release in normal myotubes involves a pathway rapidly activated by depolarization and rapidly deactivated by repolarization and that (*b*) when calcium released via this primary pathway exceeds a threshold level, it induces a secondary, regenerative release which is manifest as the slow phase of increase of the intracellular calcium transient (García and Beam, 1994).

The calcium transients in pCARD1-injected myotubes had a similar time course for test potentials of varying size, although the amplitude of the transient was larger for the test pulse to $+40$ mV than at either 0 or $+90$ mV. The variation in amplitude correlates with the integral of calcium current (during the test pulse and after repolarization), which was larger at $+40$ than at 0 or $+90$ mV (cf Fig. 4). This is the behavior expected if the calcium transient in pCARD1-injected cells is triggered by calcium entry. The cell illustrated in Fig. 6 *B* was typical of pCARD1-injected myotubes in that the calcium transients did not display the phase of slow increase that was present in calcium transients elicited by strong depolarizations applied to pCAC6-injected myotubes (Fig. 6 *A*). If it is correct that this slow phase in pCAC6-injected myotubes represents a secondary, regenerative release, the absence of a slow phase in the transients of pCARD1-injected myotubes could be explained if the intracellular calcium concentration failed to reach threshold for inducing this secondary release. Consistent with this explanation, the smaller amplitude transients in pCAC6-injected myotubes, which were typically evoked by weak depolarizations (e.g., -10 mV in Fig. 6 *A*), had a time course similar to that of the transients in pCARD1-injected myotubes (Fig. 6 *B*).

Simultaneous Measurement of Calcium Transients and Charge Movements

After completion of the simultaneous measurements of calcium transients and calcium currents in a cell, calcium channel ionic currents were blocked by the addition of $\text{Cd}^{2+} + \text{La}^{3+}$ to the bath to allow the simultaneous measurement of calcium transients and intramembrane charge movements. In order to isolate the immobilization-resistant charge movement that is thought to arise predominantly from DHP receptors, voltage clamp commands were based on the prepulse protocol

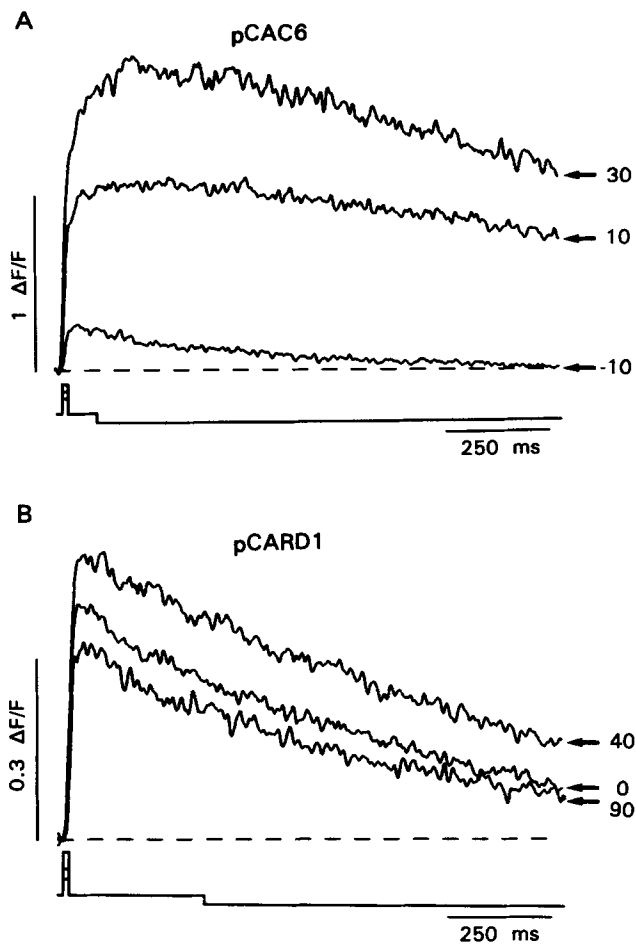


FIGURE 6. Long time-base recordings of calcium transients restored in dysgenic myotubes by pCAC6 (*A*) and pCARD1 (*B*). As in the other figures, the duration of the test pulses was 15 ms. The onset of the test pulses occurred 12.5 ms from the beginning of the illustrated transients. In *A*, note that the transient continues to increase after repolarization from the test depolarization of either +10 or +30 mV. In *B*, note that the calcium transient for the test pulse to +90 mV is caused by calcium entering the cell during the tail current produced by repolarization to -50 mV (cf Fig. 4*A*). Also note the transients decay more rapidly than those of the pCAC6-injected myotube, a difference that was consistently observed. For both *A* and *B*, the test pulses are schematically illustrated below the transients. The potential preceding and following the test pulses was -50 mV and the last downward step indicates repolarization back to the holding potential of -80 mV.

(Adams et al., 1990). The immobilization-resistant charge movements in normal myotubes and in dysgenic myotubes injected with pCAC6 or pCARD1 were qualitatively similar (Fig. 7): depolarization caused a transient, outward movement of charge ("ON" transient) and repolarization caused a comparably-sized, transient, inward movement of charge. Note that for both normal and pCAC6-injected myotubes, (*a*) stronger depolarizations were required to elicit a calcium transient than those

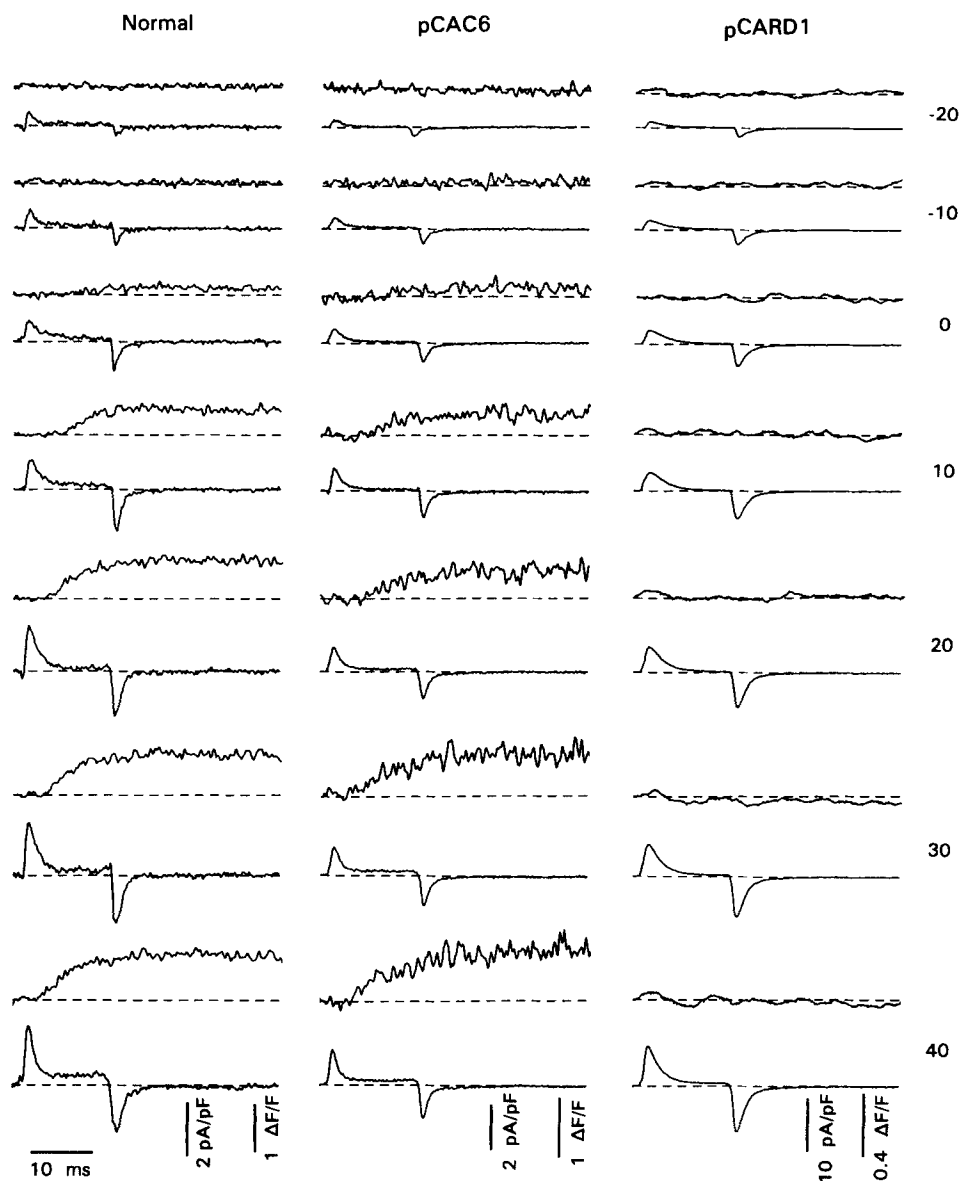


FIGURE 7. Charge movements and calcium transients in normal and injected dysgenic myotubes. Calcium transients (upper trace of each pair) and charge movements (lower trace of each pair) were recorded, after addition of $\text{Cd}^{2+} + \text{La}^{3+}$ to the external solution, from normal myotubes (*left*), pCAC6-injected myotubes (*middle*), and pCARD1-injected myotubes (*right*). The transients in normal and pCAC6-injected myotubes were qualitatively similar to those recorded before addition of $\text{Cd}^{2+} + \text{La}^{3+}$ to the bath; the transient in pCARD1-injected cells was abolished by this addition. For normal and pCAC6-injected myotubes, note that charge movement was detectable for weaker depolarizations than those needed to elicit a calcium transient and that the rising phase of the calcium transient lags the rising phase of the ON charge movement.

required for charge movement, and (b) that for a given test pulse the calcium transient begins to rise only after most of the charge has moved. To obtain a quantitative description of the immobilization-resistant charge movements, values of Q were determined by integrating the "ON" transient at each test potential (V) and fitted according to

$$Q = Q_{\max} / [1 + \exp \{(V_{Q^{1/2}} - V) / k_Q\}], \quad (3)$$

where Q_{\max} is the maximum ON charge movement, $V_{Q^{1/2}}$ is the test potential at which Q is half-maximal and k_Q is a steepness factor. Values obtained for these parameters in normal, pCAC6-injected and pCARD1-injected myotubes are summarized in Table I.

In agreement with previous results (Adams et al., 1990; Shimahara et al., 1990) control (noninjected) dysgenic myotubes display intramembrane charge movements which are smaller in amplitude than those of normal myotubes (compare Figs. 1 and 2). The immobilization-resistant charge movements of non-injected dysgenic myotubes (Q_{dys}) was measured in a total of nine cells and fitted according to Eq. 3, yielding average values of $Q_{\text{dys-max}} = 1.8 \pm 0.2 \text{ nC}/\mu\text{F}$, $k_Q = 13.3 \pm 1.3 \text{ mV}$, and $V_{Q^{1/2}} = -11.2 \pm 2.8 \text{ mV}$. In normal and pCARD1-injected myotubes, Q_{\max} (Table I) was 2.8-fold and 7.6-fold larger than $Q_{\text{dys-max}}$, respectively. In pCAC6-injected myotubes, Q_{\max} was $3.3 \pm 0.5 \text{ nC}/\mu\text{F}$ ($n = 10$), a value only 1.8-fold larger than $Q_{\text{dys-max}}$. In these cells, it seems likely that Q_{dys} represents an appreciable fraction of the total immobilization-resistant charge movement. Thus, to reduce the possible influence of contamination by Q_{dys} on the charge movement parameters in pCAC6-injected cells, data given in Table I were averaged only for those cells expressing $Q_{\max} > 3.5 \text{ nC}/\mu\text{F}$ ($n = 4$). For these four cells, $V_{Q^{1/2}}$ was $-3.5 \pm 3.8 \text{ mV}$, whereas $V_{Q^{1/2}}$ averaged $-9.3 \pm 2.5 \text{ mV}$ for the entire group of ten pCAC6-injected cells. This latter value is quite close to the value of $V_{Q^{1/2}}$ in non-injected dysgenic cells (see above).

The average value of Q_{\max} found in the present experiments for normal and pCAC6-injected myotubes are somewhat smaller than the values reported previously by Adams et al. (1990). One like explanation for this difference is that the pipette solution used for the measurements described here contained only 0.1 mM EGTA instead of the 10 mM used in the earlier work. This lower concentration of EGTA, which was employed in order to minimize interference with the intracellular processes of calcium release and reuptake, permitted the cells to contract vigorously. Because such vigorous contractions tended to dislodge the patch pipette, the use of a lower EGTA concentration probably biased our experiments towards cells expressing fewer DHP receptors and thus a smaller Q_{\max} .

As expected from earlier work demonstrating that electrically evoked contractions are abolished in pCARD1-injected myotubes by manipulations that block the restored calcium current (Tanabe et al., 1990a), the addition of $\text{Cd}^{2+} + \text{La}^{3+}$ to the bath completely eliminated the calcium transients in pCARD1-injected myotubes (Fig. 7, right hand column). The addition of extracellular $\text{Cd}^{2+} + \text{La}^{3+}$ did not produce such pronounced alterations of calcium transients in normal and pCAC6-injected myotubes (compare the left hand and center columns of Fig. 7 with Figs. 1 and 3).

However, in both normal and pCAC6-injected myotubes exposed to these calcium channel blockers, the maximal amplitude of the calcium transient was reduced (Table I, columns 4 and 10) and the decay of the transient (measured on a longer time-base) was accelerated (not shown). Similar effects of $\text{Cd}^{2+} + \text{La}^{3+}$ on calcium transients of normal myotubes were described in the previous paper (García and Beam, 1994; cf Fig. 6 A). In that paper, it was concluded that these effects were unrelated to block of calcium current.

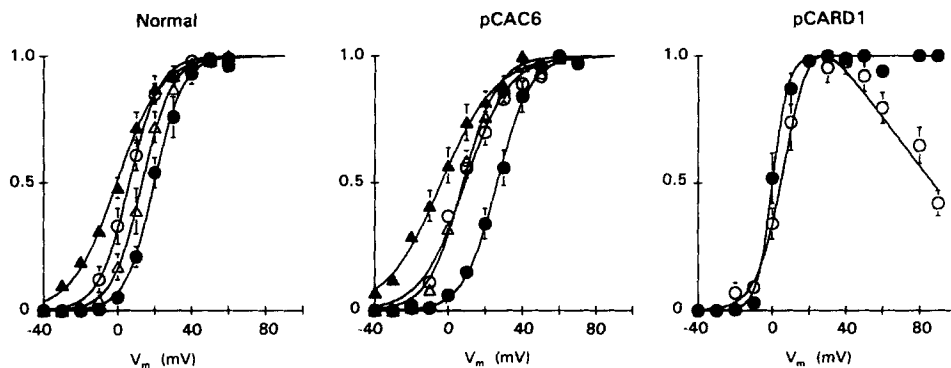


FIGURE 8. Comparison of the voltage dependence of charge movement, calcium transient and calcium current in normal and injected myotubes. For normal myotubes (*left*), pCAC6-injected myotubes (*center*) and pCARD1-injected myotubes (*right*), the quantity of ON charge moved (\blacktriangle), slow calcium channel conductance (\bullet), and the amplitude of the calcium transient measured before (\circ) or after the addition of $\text{Cd}^{2+} + \text{La}^{3+}$ to the bath (\triangle), are plotted as a function of test potential. As described in the text, only calcium conductance and calcium transient are shown for pCARD1-injected myotubes. The ON charge and $\Delta F/F$ data were normalized by the maximum value of the respective parameter for each cell and averaged. The averaged data were then fitted by Eqs. 2 and 3 as appropriate. For pCAC6-injected cells, the averages reflect data only from cells with $Q_{\text{max}} > 3.5 \text{ nC}/\mu\text{F}$. To obtain calcium conductance, peak $I_{\text{Ca}}-V$ data for each cell were fitted with Eq. 1 to obtain V_{rev} and values of conductance were calculated as $G_{\text{Ca}}(V) = I_{\text{Ca}}(V)/(V - V_{\text{rev}})$ and normalized by G'_{max} for that cell (normal and pCAC6-injected) or by the average value of G_{Ca} for $V_m \geq 30 \text{ mV}$ (pCARD1-injected). The normalized values of G_{Ca} were then averaged and fitted according to $G_{\text{Ca}}(V) = G'_{\text{max}}/[1 + \exp\{(V_{\text{G}^{1/2}} - V)/k'_{\text{G}}\}]$. The midpoint ($V_{1/2}$) and steepness (k) parameters for the smooth curves for normal and pCAC6-injected myotubes, respectively, are: Q_{ON} , -0.6 mV and 11.9 mV , -3.8 mV and 14.9 mV ; $\Delta F/F$, 6.3 mV and 8.2 mV , 9.2 mV and 11.8 mV ; $\Delta F/F$ ($\text{Cd}^{2+} + \text{La}^{3+}$ in bath), 13.3 mV and 8.1 mV ; 8.1 mV and 9.4 mV ; G_{Ca} , 19.8 mV and 7.7 mV ; 26.41 mV and 8.9 mV . For the pCARD1-injected myotubes, $V'_{\text{G}^{1/2}}$ and k'_{G} were 0.15 mV and 4.14 mV , respectively.

Relationship Between Charge Movement, Calcium Transient and Calcium Current in Normal and Injected Myotubes

Fig. 8 illustrates, for both normal myotubes (*left*) and pCAC6-injected dysgenic myotubes (*center*), the voltage dependence of charge movement (\blacktriangle), slow calcium channel conductance (\bullet), and the calcium transient measured before (\circ) or after (\triangle)

the addition of $\text{Cd}^{2+} + \text{La}^{3+}$. To allow averaging of data from different cells, the values for charge, fluorescence change and conductance from an individual cell were normalized to the maximum value of that parameter. The smooth curves through the data points for the slow calcium conductance, calcium transient and charge movement represent least-squares fits of Eqs. 1, 2, and 3, respectively. Average values of the parameters determined by fits of these equations to data from individual cells are summarized in Table I.

In those pCARD1-injected myotubes where both calcium current and charge movement were successfully measured, the expressed calcium current was sufficiently large (see above) that estimated series resistance errors were no less than 8 mV and in some cases much larger. As a result, comparison of the voltage dependence of the slow calcium conductance and of charge movement (made after block of the calcium current) is severely compromised because the total current flow, and attendant series resistance error, is very different for the two kinds of measurements. Thus, for the pCARD1-injected myotubes, only the slow calcium conductance and the calcium transient measured before addition of $\text{Cd}^{2+} + \text{La}^{3+}$ are shown (Fig. 8, *right*) because these were measured under comparable conditions. Note that the rising phase of the curve relating the calcium transient to voltage nearly superimposes on the curve of calcium conductance vs voltage, as expected if the transient in pCARD1-injected cells is triggered by calcium entering through the calcium channel.

The curves relating charge movement to test potential are very similar for normal and pCAC6-injected myotubes, as are the curves relating calcium transients to test potential (Fig. 8, Table I). Specifically, for both normal and pCAC6-injected cells, the curves for calcium transient vs potential are steeper than the corresponding Q - V curves and shifted to the right. The G - V curves are shifted still farther to the right, with the shift ($V_{G1/2} - V_{Q1/2}$) being 15.6 and 27.5 mV for normal and pCAC6-injected myotubes, respectively. A value of $V_{G1/2} - V_{Q1/2}$ that was larger in pCAC6-injected myotubes than in normal myotubes has been described previously (Adams et al., 1990). Despite the fact that the activation of calcium conductance has an altered relationship to charge movement in pCAC6-injected myotubes compared to normal myotubes, the functional relationship between calcium transient and charge movement is similar in pCAC6-injected and normal myotubes (Figs. 7 and 8).

After the addition of $\text{Cd}^{2+} + \text{La}^{3+}$, the curve relating the calcium transient to voltage for normal myotubes was shifted slightly to the right (Fig. 8, Table I). We are uncertain as to the reason for this phenomenon. One possibility is that the shift results from a time-dependent change in the properties of the myotube, because the measurements with the heavy metals were always made later in the experiment. Alternatively, the shift may be a consequence of the heavy metals entering the cell. In support of the latter possibility, we noted that the addition of the heavy metals caused an increase in basal fluorescence which occurred more rapidly in cells expressing higher densities of slow calcium current. The fact that pCAC6-injected myotubes express a lower density of slow calcium current than normal myotubes may explain why there was no shift of the curve relating the transient to voltage for injected myotubes.

DISCUSSION

pCAC6- and pCARD1-injected Myotubes Mimic e-c Coupling of Skeletal or Cardiac Muscle, Respectively

In this paper, we have compared the properties of intracellular calcium transients, calcium currents and intramembrane charge movements measured simultaneously with fluorometry and whole-cell patch clamping in normal myotubes and dysgenic myotubes injected with pCAC6 or pCARD1, cDNAs encoding the skeletal muscle or cardiac DHP receptor, respectively. In both normal and pCAC6-injected myotubes, the amplitude of the calcium transient increased sigmoidally as a function of test potential, saturating for strong depolarization. Also in both types of myotubes, an intracellular calcium transient was still present after block of the DHP-sensitive current. Thus, both the endogenous and expressed skeletal muscle DHP receptor are able to function as a voltage sensor which can elicit the release of calcium from the SR in a direct fashion that does not require the entry of extracellular calcium. In this respect, as well as in respect to the inter-relationships between charge movement, calcium transient and calcium current, normal and pCAC6-injected myotubes resemble adult frog skeletal muscle fibers (Chandler et al., 1976; Miledi, Parker, and Zhu, 1984; Melzer, Schneider, Simon, and Szücs, 1986; Brum, Stefani, and Ríos, 1987; Simon and Schneider, 1988; García, Amador, and Stefani, 1989).

In dysgenic myotubes injected with pCARD1, the amplitude of the calcium transient showed a bell-shaped dependence on test potential, mirroring the amplitude of the DHP-sensitive current. Blocking the calcium current, completely abolished the calcium transient in pCARD1-injected myotubes. Several lines of evidence support the idea that the calcium transient in pCARD1-injected myotubes predominantly reflects calcium released from the SR, rather than just resulting from the entry of external calcium. First, some pCARD1-injected cells display large calcium currents (Fig. 4 B, see below) but no detectable transient or electrically-evoked contraction. Second, we have previously shown that following caffeine treatments, expected to deplete partially the SR of calcium, contractions become stronger with successive, identical voltage-clamp commands even though the amplitude of the calcium current remained constant (Tanabe et al., 1990a). Taken together, these observations support the idea that the cardiac DHP receptor expressed in dysgenic myotubes is unable to function as a voltage sensor but is able to function as a calcium channel, which elicits calcium-induced calcium release from the SR. Thus, pCARD1-injected myotubes mimic cardiac muscle cells (Fabiato, 1985; Näbauer et al., 1989).

Presence of Calcium Current in Noncontracting Myotubes

Interestingly, some dysgenic myotubes injected with pCAC6 or pCARD1 expressed significant calcium current but did not show electrically evoked contractions and/or an appreciable calcium transient. For example, out of 48 dysgenic cells injected with pCAC6 (three separate cultures), 14 were found to contract and all of these expressed slowly activating calcium current, with an average peak density of -3.9 ± 0.8 pA/pF. Of the 34 noncontracting cells, 28 did not express measurable slow calcium current. However, six of these noncontracting cells expressed slowly activating calcium current at an appreciable level (-2.0 ± 0.5 pA/pF). Thus, with the exception of a few

cells, the expressed skeletal DHP receptor functioned both as a calcium channel and as a voltage sensor. Perhaps, in the cells expressing current but no contraction, the newly synthesized DHP receptors were not localized correctly with respect to, or had not yet established a functional connection with, the calcium release channel of the SR. However, we cannot exclude the possibility that the failure to contract was due to immaturity of the SR or contractile apparatus. Compared to dysgenic myotubes transfected with pCAC6, many more of those transfected with pCARD1 expressed current but not electrically-evoked contraction. Although not examined systematically, we did observe in two separate cultures that about half of the dysgenic myotubes transfected with pCARD1 by CaPO₄ precipitation (Chen and Okayama, 1988) displayed appreciable cardiac-like calcium current (-12.6 ± 2.5 pA/pF, $n = 8$) but did not contract. An example of a pCARD1-injected myotube expressing large calcium current but no calcium transient is illustrated in Fig. 4 B. The observation of a higher fraction of noncontracting myotubes expressing cardiac calcium current than of noncontracting myotubes expressing skeletal muscle calcium current may indicate that the process that directs the co-localization of the DHP receptor and the release channel is more tightly coupled for the skeletal muscle DHP receptor than for the cardiac DHP receptor.

A Simple Model for the Function of a DHP Receptor as Voltage Sensor and Calcium Channel

Based on the data presented in this paper on normal and injected myotubes, on similar data obtained from fibers of adult frog skeletal muscle (Chandler et al., 1976; Melzer et al., 1986; Brum et al., 1987; Simon and Schneider, 1988; García et al., 1989), and experimental analysis of chimaeric DHP receptors (Tanabe et al., 1990b; Tanabe, Adams, Numa, and Beam, 1991), we present the model in Fig. 9. The model is suggested as a simple scheme in which conformational changes of an individual DHP receptor can account for the inter-relationships, in both time and voltage dependence, between charge movement, calcium transient and slow calcium current. For simplicity, the model shows the ryanodine receptor (RyR), the putative SR release channel (Fleischer, Ogunbunmi, Dixon, and Fleer, 1985; Lai, Erickson, Rousseau, Liu, and Meissner, 1988; Smith, Imagawa, Ma, Fill, Campbell, and Coronado, 1988), as interacting with a single DHP receptor, although both morphological (Block, Imagawa, Campbell, and Franzini-Armstrong, 1988) and physiological (Simon and Hill, 1992) analyses are consistent with the idea that activation of calcium release is controlled cooperatively by four DHP receptors (one DHP receptor interacting with each of the four subunits of the RyR).

In the model, the opening and closing of the RyR is controlled by the conformational state of the putative cytoplasmic loop (the "II-III loop") linking repeats II and III of the DHP receptor, an idea motivated by previous work in which putative cytoplasmic regions of the cardiac DHP receptor were replaced by corresponding regions of the skeletal muscle DHP receptor (Tanabe et al., 1990b). However, other cytoplasmic regions might also interact with the RyR. Such regions probably would not have been revealed by the experiments of Tanabe et al. (1990b) if their amino acid sequence were similar in the skeletal and cardiac muscle DHP receptors. Based on the observation that channel activation is slow whenever repeat I of a skeletal/

cardiac chimaeric DHP receptor has skeletal muscle sequence (Tanabe et al., 1991), repeat I is illustrated as the last to undergo a conformational change in order to open the channel. Determining the voltage dependence of this conformational change will require single channel measurements. A model in which a conformational change of repeat I is rate-limiting for channel opening has been used by Feldmeyer, Melzer, Pohl, and Zöllner (1992) to account for the effects of strongly depolarizing prepulses on kinetics of activation of calcium current in frog skeletal muscle.

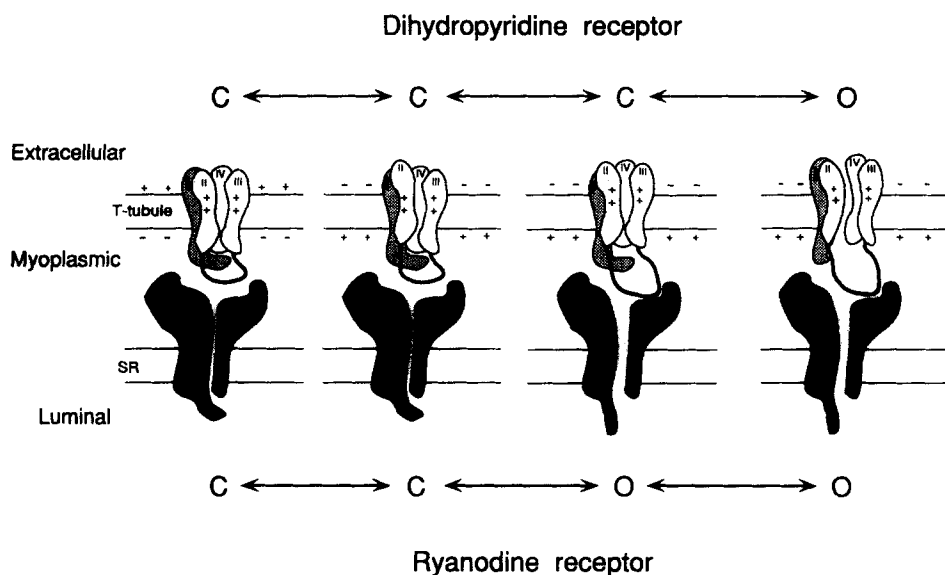


FIGURE 9. A simple model of the DHP receptor functioning as both a voltage sensor and a calcium channel. The model depicts the DHP receptor within the T-tubule membrane and the ryanodine receptor in the neighboring SR membrane. The four homology repeats (Tanabe et al., 1987) are indicated by Roman numerals; for simplicity, the homotetrameric structure (Lai et al., 1988; Wagenknecht, Grassucci, Frank, Saito, Inui, and Fleischer, 1989) of the ryanodine receptor is not shown. Plus signs on the DHP receptor are meant to indicate the presence of positively charged residues (Tanabe et al., 1987). The leftmost panel indicates the resting state in which the myoplasmic face of the T-tubule is polarized negatively with respect to the extracellular face. The rightmost three panels illustrate conformational alterations of the DHP receptor and ryanodine receptor that are caused by T-tubular depolarization. Closed (C) and open (O) states are indicated both for the dihydropyridine receptor and the ryanodine receptor. For further details, see text.

The model in Fig. 9 can account for important experimental observations on the interrelationships between charge movement, calcium transient and calcium current. The leftmost state represents the resting configurations and both the DHP receptor and the RyR are closed to the flow of ions. Upon depolarization, the system undergoes a sequence of conformation changes proceeding from left to right. The initial voltage-driven conformational change (movement from leftmost state to adjoining state) is arbitrarily illustrated as occurring in repeat II. This conformational

change (illustrated as a simple translocation across the T-tubule membrane) would generate intramembrane charge movement but would not cause the altered configuration of the II-III loop necessary to open the RyR. Thus, this conformational change is one way to account for the movement of charge that precedes intracellular calcium release temporally (see Figs. 1 and 3) and for the charge that moves for weaker depolarizations than required to elicit calcium release (Fig. 8). When both repeats II and III have undergone a voltage-driven conformational change (third state from left), the altered configuration of the II-III loop causes the RyR to open, although the DHP-sensitive channel is still closed. (For simplicity, the conformational change of repeat IV is shown to occur simultaneously with that of repeat III). Finally, a conformational change in repeat I causes the channel to open. Thus, channel opening occurs later in time, and requires stronger depolarization, than the activation of the RyR (Figs. 1, 3, and 8).

Although the model of Fig. 9 is incomplete, it is useful in that it summarizes many experimental observations and in that it provides a conceptual framework for future experiments. For example, it predicts that mutations introduced into repeat I could affect the voltage dependence and kinetics of calcium current with little or no effect on calcium release. Mutations introduced into repeats II or III would be expected to most strongly affect voltage dependence and/or kinetics of charge movements and calcium transients, with much less effect on the current.

We thank Lorrie Bennett, Aaron Beam, and Jennifer Hanneman for their technical assistance.

This work was supported by research grants NS24444 and NS28323 from the NIH, and partially by a Postdoctoral Fellowship to J. García from the American Heart Association of Colorado.

Original version received 21 May 1993 and accepted version received 24 August 1993.

REFERENCES

- Adams, B. A., and K. G. Beam. 1989. A novel calcium current in dysgenic skeletal muscle. *Journal of General Physiology*. 94:429–444.
- Adams, B. A., and K. G. Beam. 1991. Contractions of dysgenic skeletal muscle triggered by a potentiated, endogenous calcium current. *Journal of General Physiology*. 97:687–696.
- Adams, B. A., T. Tanabe, A. Mikami, S. Numa, and K. G. Beam. 1990. Intramembrane charge movement restored in dysgenic skeletal muscle by injection of dihydropyridine receptor cDNAs. *Nature*. 346:569–572.
- Beam, K. G., and J. García. 1993. Ca^{2+} transients, Ca^{2+} current and charge movement in cultured skeletal muscle. *Biophysical Journal*. 64:241a. (Abstr.)
- Beam, K. G., C. M. Knudson, and J. A. Powell. 1986. A lethal mutation in mice eliminates the slow calcium current in skeletal muscle cells. *Nature*. 320:168–170.
- Beuckelmann, D. J., and W. G. Wier. 1988. Mechanism of release of calcium from sarcoplasmic reticulum of guinea-pig cardiac cells. *Journal of Physiology*. 405:233–235.
- Block, B. A., T. Imagawa, K. P. Campbell, and C. Franzini-Armstrong. 1988. Structural evidence for direct interaction between the molecular components of the transverse tubule/sarcoplasmic reticulum junction in skeletal muscle. *Journal of Cell Biology*. 107:2587–2600.
- Brum, G., E. Stefani, and E. Ríos. 1987. Simultaneous measurements of Ca^{2+} currents and intracellular Ca^{2+} concentrations in single skeletal muscle fibers of the frog. *Canadian Journal of Physiology and Pharmacology*. 65:681–685.

- Chandler, W. K., R. F. Rakowski, and M. F. Schneider. 1976. Effects of glycerol treatment and maintained depolarization on charge movement in muscle. *Journal of Physiology*. 254:285–316.
- Chaudhari, N. 1992. A single nucleotide deletion in the skeletal muscle-specific calcium channel transcript of muscular dysgenesis (*mdg*) mice. *Journal of Biological Chemistry*. 267:25636–25639.
- Chen, C. A., and H. Okayama. 1988. Calcium phosphate-mediated gene transfer: a highly efficient transfection system for stably transforming cells with plasmid DNA. *Biotechniques*. 6:632–638.
- Fabiato, A. 1985. Time and calcium dependence of activation and inactivation of calcium-induced release of calcium from the sarcoplasmic reticulum of a skinned canine cardiac purkinje cell. *Journal of General Physiology*. 85:247–290.
- Feldmeyer, D., W. Melzer, B. Pohl, and P. Zöllner. 1992. Modulation of calcium current gating in frog skeletal muscle by conditioning depolarization. *Journal of Physiology*. 457:639–653.
- Fleischer, S., E. M. Ogunbunmi, M. C. Dixon, and E. A. M. Fleer. 1985. Localization of Ca²⁺ release channels with ryanodine in junctional terminal cisternae of sarcoplasmic reticulum of fast skeletal muscle. *Proceedings of the National Academy of Sciences, USA*. 82:7256–7259.
- García, J., M. Amador, and E. Stefani. 1989. Relationship between myoplasmic calcium and calcium currents in frog skeletal muscle. *Journal of General Physiology*. 94:973–986.
- García, J., and K. G. Beam. 1994. Measurement of calcium transients and slow calcium current in myotubes. *Journal of General Physiology*. 103:107–123.
- García, J., T. Tanabe, and K. G. Beam. 1993. Comparison of Ca²⁺ transients in dysgenic myotubes expressing skeletal and cardiac DHP receptors. *Biophysical Journal*. 64:241a. (Abstr.)
- Gluecksohn-Waelsch, S. 1963. Lethal genes and analysis of differentiation. *Science*. 142:1269–1276.
- Hamill, O. P., A. Marty, E. Neher, B. Sakmann, and F. J. Sigworth. 1981. Improved patch-clamp techniques for high-resolution current recording from cells and cell-free membrane patches. *Pflügers Archiv*. 391:85–100.
- Klaus, M. M., S. P. Scordilis, J. M. Rapalus, R. T. Briggs, and J. A. Powell. 1983. Evidence for dysfunction in the regulation of cytosolic Ca²⁺ in excitation-contraction uncoupled dysgenic muscle. *Developmental Biology*. 99:152–166.
- Knudson, C. M., N. Chaudhari, A. H. Sharp, J. A. Powell, K. G. Beam, and K. P. Campbell. 1989. Specific absence of the α_1 subunit of the dihydropyridine receptor in mice with muscular dysgenesis. *Journal of Biological Chemistry*. 264:1345–1348.
- Lai, F. A., H. P. Erickson, E. Rousseau, Q.-Y. Liu, and G. Meissner. 1988. Purification and reconstitution of the calcium release channel from skeletal muscle. *Nature*. 331:315–319.
- Melzer, W., M. F. Schneider, B. J. Simon, and G. Szücs. 1986. Intramembrane charge movement and calcium release in frog skeletal muscle. *Journal of Physiology*. 373:481–511.
- Mikami, A., K. Imoto, T. Tanabe, T. Niidome, Y. Mori, H. Takeshima, S. Narumiya, and S. Numa. 1989. Primary structure and functional expression of the cardiac dihydropyridine-sensitive calcium channel. *Nature*. 340:230–233.
- Miledi, R., I. Parker, and P. H. Zhu. 1984. Extracellular ions and excitation-contraction coupling in frog twitch muscle fibres. *Journal of Physiology*. 351:687–710.
- Näbauer, M., G. Callewaert, L. Cleemann, and M. Morad. 1989. Regulation of calcium release is gated by calcium current, not gating charge, in cardiac myocytes. *Science*. 244:800–803.
- Powell, J. A., and D. M. Fambrough. 1973. Electrical properties of normal and dysgenic mouse skeletal muscle in culture. *Journal of Cell Physiology*. 82:21–38.
- Ríos, E., and G. Brum. 1987. Involvement of dihydropyridine receptors in excitation-contraction coupling in skeletal muscle. *Nature*. 325:717–720.
- Schneider, M. F., and W. K. Chandler. 1973. Voltage dependent charge movement in skeletal muscle: a possible step in excitation-contraction coupling. *Nature*. 242:244–246.

- Shimahara, T., R. Bornaud, I. Inoue, and C. Strube. 1990. Reduced intramembrane charge movement in the dysgenic skeletal muscle cell. *Pflügers Archiv.* 417:111–113.
- Simon, B. J., and D. A. Hill. 1992. Charge movement and SR calcium release in frog skeletal muscle can be related by a Hodgkin-Huxley model with four gating particles. *Biophysical Journal.* 61:1109–1116.
- Simon, B. J., and M. F. Schneider. 1988. Time course of activation of calcium release from sarcoplasmic reticulum in skeletal muscle. *Biophysical Journal.* 54:1159–1163.
- Smith, J. S., T. Imagawa, J. Ma, M. Fill, K. P. Campbell, and R. Coronado. 1988. Purified ryanodine receptor from rabbit skeletal muscle is the calcium-release channel of sarcoplasmic reticulum. *Journal of General Physiology.* 92:1–26.
- Tanabe, T., K. G. Beam, J. A. Powell, and S. Numa. 1988. Restoration of excitation-contraction coupling and slow calcium current in dysgenic muscle by dihydropyridine receptor complementary DNA. *Nature.* 336:134–139.
- Tanabe, T., A. Mikami, S. Numa, and K. G. Beam. 1990a. Cardiac-type excitation-contraction coupling in dysgenic skeletal muscle injected with cardiac dihydropyridine receptor cDNA. *Nature.* 344:451–453.
- Tanabe, T., K. G. Beam, B. A. Adams, T. Niidome, and S. Numa. 1990b. Regions of the skeletal muscle dihydropyridine receptor critical for excitation-contraction coupling. *Nature.* 346:567–569.
- Tanabe, T., B. A. Adams, S. Numa, and K. G. Beam. 1991. Repeat I of the dihydropyridine receptor is critical in determining calcium channel activation kinetics. *Nature.* 352:800–803.
- Wagenknecht, T., R. Grassucci, J. Frank, A. Saito, M. Inui, and S. Fleischer. 1989. Three-dimensional architecture of the calcium channel/foot structure of sarcoplasmic reticulum. *Nature.* 338:167–170.
- Wier, W. G. 1990. Cytoplasmic [Ca²⁺] in mammalian ventricle: dynamic control by cellular processes. *Annual Review of Physiology.* 52:467–485.